RESEARCH ARTICLE
doi: 10.2306/scienceasia1513-1874.2026.041

ScienceAsia 52 (2): 2026: ID 2026041: **1–13**

Effects of *Sanghuangporus vaninii* and *Calvatia gigantea* polysaccharide hydrogels on DNFB-induced atopic dermatitis in mice

Wei Li[a], Wenzhe Wang[a], Yukai Zhang[b,c], Chunhe Guo[a], Hong Ji[a], Jiaxuan Wang[a], Lu Fu[a,c,*]

[a] Engineering Research Center of Bioreactor and Pharmaceutical Development, Ministry of Education, College of Life Science, Jilin Agricultural University, Changchun 130118 China
[b] Neurosurgery Department, The Second Hospital of Jilin University, Changchun 130000 China
[c] JiLin Ferry Innovation Factory Group, Changchun 130012 China

[*]Corresponding author, e-mail: f837615056@126.com

Received 3 Jun 2025, Accepted 21 Apr 2026
Available online 18 May 2026

ABSTRACT: Atopic dermatitis (AD), a chronic inflammatory skin disorder that affects more than 20% of children and 10% of adults globally, requires novel therapeutic strategies. *Sanghuangporus vaninii* (*S. vaninii*) and *Calvatia gigantea* (*C. gigantea*) are medicinal fungi that have anti-inflammatory and immunomodulatory properties. In this study, we extracted and purified the total polysaccharides of *S. vaninii* (SVP) and *C. gigantea* (CGP) and prepared two types of polysaccharide-based hydrogels for AD treatment. The hydrogels exhibited porous microstructures and high hydration capacities. In a standardized 2,4-dinitrofluorobenzene (DNFB)-induced AD mouse model, both SVP and CGP-hydrogels demonstrated significant therapeutic efficacy, with SVP showing a more pronounced effect. The SVP and CGP-hydrogels reduced dermatitis scores and ear thickness after a 14-day treatment period. Histopathological analysis revealed that SVP and CGP-hydrogels suppressed epidermal hyperplasia and mast cell infiltration. RT-qPCR and Elisa analysis showed that SVP and CGP-hydrogels significantly downregulated the express levels of pro-inflammatory cytokines (TNF-α, IL-1β and IL-6) and upregulated the anti-inflammatory cytokines IL-10. Notably, SVP-hydrogel could affect the expression levels of Th1 and Th2 cell-specific cytokines in AD mice, suggesting that SVP may be used to treat AD by restoring immune balance. These findings indicate that SVP and CGP-hydrogels are promising adjuvant therapies for AD.

KEYWORDS: atopic dermatitis, *Sanghuangporus vaninii* polysaccharide, *Calvatia gigantea* polysaccharide, hydrogel

INTRODUCTION

Atopic dermatitis (AD), clinically termed atopic eczema, is one of the most common chronic inflammatory skin disorders, affecting about 20% of the pediatric population and 10% of adults in developed nations [1]. AD is characterized by recurrent eczematous lesions, such as erythema, papules, and exudative lesions, in specific areas. These pathological lesions severely impair sleep quality and also impose substantial burdens on daily functioning and occupational productivity [2]. The pathogenesis of AD is complex and involves interactions among genetic predisposition, environmental triggers, epidermal barrier dysfunction (e.g., filaggrin mutations), immune system dysregulation (Th1/Th2 imbalance), and cutaneous microbiome alterations. Notably, CD4+ T lymphocyte infiltration and the Th1/Th2 cytokine ratio are critical biomarkers for evaluating disease progression and therapeutic outcomes in AD management [3].

Common therapeutic strategies for AD include oral antihistamines, glucocorticoids, and calcineurin phosphatase inhibitors. However, they can cause irreversible side effects such as capillary dilation and hyperpigmentation. Emerging biological agents that target AD, such as Interleukin (IL-4)/IL-13 (dupilumab) and JAK-STAT pathway inhibitors, have expanded treatment options [4]. However, these interventions are also associated with adverse events, drug tolerance, and long-term use-induced conjunctivitis or thromboembolism, which requires the exploration of safer therapeutic alternatives with multitargeted mechanisms of action [5]. Accumulating evidence has shown that natural polysaccharides have significant therapeutic potential for modulating inflammatory responses and maintaining immune homeostasis. Notably, polysaccharides isolated from *Ganoderma lucidum*, *Houttuynia cordata*, and *Lonicera japonica* have been shown to alleviate AD symptoms [6–8]. These natural polysaccharides offer distinct advantages over traditional immunosuppressants due to their complex chemical compositions and multitarget mechanisms of action. Natural polysaccharides for AD treatment can reduce the risk of drug resistance, produce fewer side effects, be applied to sensitive skin, and reduce the financial burden on patients [9].

Sanghuangporus vaninii (*S. vaninii*) is a large perennial medicinal fungus that belongs to the Hymenochaetaceae family and is mainly distributed in Asian countries. The earliest record of its medicinal applications dates back to *Shennong's Herbal Classic of Materia Medica* in 2000 BCE [10]. This fungus has historically been used in traditional Chinese medicine as a culinary and therapeutic agent to manage diverse conditions, including hemorrhagic disorders, gastrointestinal diseases, and age-related de-

generation [11]. Pharmacological investigations into *S. vaninii* polysaccharide (SVP) have revealed a wide range of anti-inflammatory, antitumor, antioxidant, antidiabetic, and immunomodulatory effects, which are beneficial in managing diabetes mellitus, rheumatoid arthritis, atherosclerosis, and other diseases.

Calvatia gigantea (*C. gigantea*) is an edible medicinal fungus in the family Calvaceae that is prevalent in various regions of the world [12]. It was first recorded in the *Miscellaneous Records of Famous Physicians* and exhibits antimicrobial, anti-inflammatory, antitussive, anticancer properties, and inhibits cell growth. Pharmacological investigations of *C. gigantea* polysaccharide (CGP) have revealed broad anti-inflammatory, antitumor, and hepatoprotective functions [13].

While AD presents clinically as cutaneous inflammation, its underlying pathophysiology involves complex immune dysregulation characterized by a Th1/Th2 imbalance and T-cell overactivation [14]. Conventional pharmacological interventions primarily alleviate symptomatic manifestations without addressing fundamental immunological perturbations. In contrast, fungus-derived polysaccharides exert synergistic therapeutic effects via dual anti-inflammatory and immunomodulatory mechanisms, as exemplified by SVP and CGP [15, 16]. Therefore, we extracted and purified SVP and CGP, and prepared two types of polysaccharide-based hydrogels for AD intervention. We evaluated the physical and chemical properties of the hydrogels and investigated their effects on mouse model of AD, to lay a foundation for developing therapeutic drugs as well as the application of fungal polysaccharides to AD.

MATERIALS AND METHODS

Extraction and purification of SVP and CGP

Fruiting bodies of *S. vaninii* collected in Changchun, China, were mechanically pulverized, and then triplicate aqueous extracts were obtained in hot water under the following optimized parameters: solid-liquid ratio 1:30 (w/v), temperature 95 ± 2 °C, 3.5 h per cycle. Aqueous extracts were combined and concentrated by rotary evaporation (55 °C, 100 mbar) to 200 ml, followed by ethanol precipitation (4 × volumes, 4 °C, 12 h). Polysaccharide-rich precipitates were recovered by centrifugation (8,000 × *g*, 15 min, 4 °C), then sequentially deproteinized using the Sevag reagent (butanol/chloroform, v/v = 1:4). Total SVP was purified by molecular dialysis (3.5 kDa MWCO, 4 °C, and distilled water was renewed every 6 h for 48 h, then lyophilized.

The optimized parameters for CGP extraction were as follows: solid-liquid ratio 1:16 (w/v), triplicate extractions at 90 ± 2 °C, for 1 h per cycle. Post-concentration (identical to SVP), ethanol precipitation (4 × volumes) yielded total CGP, which was deproteinized, dialyzed, and lyophilized as described above.

Ultraviolet (UV) spectral analysis

Protein and nucleic acid contaminants in two polysaccharide samples were detected using UV spectroscopy. Absorbance spectra from 200 to 600 nm were analyzed by a UV-Vis spectrophotometer (Multiskan GO, Thermo Fisher Scientific Inc., Waltham, MA, USA), with distilled water as the reference.

FT-IR spectroscopy analysis

Polysaccharide spectra were acquired using a Nicolet IS50 FT-IR spectrometer (Thermo Fisher Scientific Inc.) as described by Wang et al with minor modifications [17]. Briefly, 1 mg of sample was blended with 100 mg of KBr powder, pressed into translucent pellets, and scanned over the wavenumber range of 4,000–500 cm^{-1}.

Scanning electron microscope (SEM) assay

Sample morphology was characterized using an SU8600 SEM (Hitachi, Ltd., Tokyo, Japan) and the Sci-go Instrumentation Testing Platform. Lyophilized samples were sputter-coated with gold for 20 min under vacuum to enhance conductivity. Micrographs were acquired at an acceleration voltage of 3.0 kV [18].

Preparation of SVP and CGP-hydrogels

Hydrogels were prepared according to established protocols with the following modifications. Carbomer 940 (0.5 g) was hydrated in ultrapure water (40 ml, 25 °C, 12 h), and 0.4 g of carboxymethyl chitosan (CMCS) was dissolved in 4 ml of water heated to 60 °C [19]. The CMCS solution (2.5 ml) was incrementally incorporated into the swollen carbomer by mechanical stirring at 500 rpm for 5 min. Sterile aqueous solutions containing 10% (w/v) SVP or CGP (calculated as polysaccharide equivalents) were prepared. Portions (6.667 ml) of polysaccharide solutions were incorporated into the hydrogel precursor and homogenized. We adjusted the pH to 6.9–7.2 by triethanolamine titration, followed by final mass adjustment to 100 g with sterile water. The resulting hydrogel was mixed with SVP or CGP (15 min, 25 °C), portioned into sterile containers, and stored at 4 °C.

Water loss rate (%) determination

Hydrogels (1 g) were placed in microtubes, and the original weight (m_0) was recorded. Samples were dehydrated in a forced-air convection oven at 37 °C for 18 h with gravimetric measurements recorded at 60-min intervals (m_a) until mass stabilization (m_b) was achieved. The cumulative water loss rate (%) was calculated as:

$$\text{Water loss rate (\%)} = (m_0 - m_a)/(m_0 - m_b) \times 100\%$$

All samples were measured in triplicate [19].

Cell viability assays

The RAW 264.7 macrophages were maintained in DMEM supplemented with 10% FBS and 1% Penicillin-Streptomycin-Amphotericin B under standard culture conditions (37 °C, 5% CO_2). Cells (1×10^4/well; 100 µl/well) were seeded in 96-well plates and incubated for 24 h. Cell viability was assessed by incubating the cells with serial concentrations of SVP/CGP (25, 50, 100, 200 µg/ml in serum-free medium) for 24 h at 37 °C. After polysaccharide stimulation, CCK-8 reagent (10 µl/well) was added, and the cells were incubated for 1 h at 37 °C. Absorbance was read at 450 nm using an Infinite® M200 pro microplate reader (TECAN Infinite M200 Pro, Männedorf, Switzerland).

Quantitation of cytokines secreted by RAW264.7 macrophages and nitric oxide

The RAW264.7 macrophages (1×10^5/well; 2 ml/well) were seeded in 6-well plates at 37 °C for 24 h under serum starvation. The cells were challenged with LPS (1 µg/ml in DMEM) for 24 h to establish an inflammatory model. The cells were then incubated with SVP/CGP (25–200 µg/ml in medium containing LPS) at 37 °C for 24 h. Conditioned media were centrifuged, then NO content in supernatants (50 µl) was quantified using Nitric Oxide Assay Kits (Beyotime Biotechnology, Shanghai, China).

The cells were washed with PBS, and then cytokines were quantified in cell suspensions. Total RNA was isolated using SevenFast® Total RNA Extraction Kits (SevenBio, Beijing, China) and DNase I. Levels of TNF-α and IL-1β pro-inflammatory cytokine transcripts were quantified by RT-qPCR (detailed below) using β-actin as the endogenous control.

Animal experiments and grouping design

Forty 6-week-old female SPF grade BALB/c mice weighing 18–22 g (Certificate No: SCXK[LN]2020-0001; Liaoning Changsheng Biotechnology Co., Ltd., Changchun, China) were housed and allowed adaptive feeding for at least one week. All procedures complied with the ARRIVE guidelines (https://arriveguidelines.org) and were approved by the Laboratory Animal Welfare and Ethics Committee of Jilin Agricultural University (permit No. 20240909017).

Fig. 1 shows the experimental procedure. The mice were randomly assigned to the following groups ($n = 8$ each): control, model, blank, SVP, and CGP hydrogels (0.667 mg/cm^2 calculated as polysaccharide equivalents) [20, 21]. After a 3×2 cm dorsal area was depilated using a razor and depilatory cream, the mice were sensitized on day 1 with 0.5% (w/v) 2,4-dinitrofluorobenzene (DNFB) (100 µl dorsal skin/25 µl right ear) in acetone-olive oil (3:1, v/v) and challenged on days 4, 7, 10, and 13 with 0.2% (w/v) DNFB in acetone-olive oil. The blank, SVP-hydrogel and CGP-hydrogel groups were treated daily from days 1 to 14, whereas controls and models received equal-volume normal saline. Skin and ear lesions were documented by high-resolution imaging. Tissues were collected from mice euthanized on day 15 by a pentobarbital overdose (100 mg/kg i.p.). Dorsal skin and ear specimens were fixed in 4% paraformaldehyde for histopathology, snap-frozen in liquid nitrogen for cytokine analysis, or preserved in RNA storage solution at −80 °C for molecular studies.

Skin inflammation and auricular edema assessment

Three blinded assessors independently evaluated dorsal skin lesions on days 1, 4, 7, 10, and 13 using a validated scoring system from 0–3 per parameter (0, absent; 1, mild (slight swelling/pale erythema/minimal excoriation/faint scaling); 2, moderate (distinct swelling/erythema with punctate hemorrhage/focal erosion/visible scaling); 3, severe (diffuse swelling/deep erythema with hemorrhage/extensive ulceration/marked scaling with crusting) [22, 23]. The sum of the four parameters (total scores) ranged from 0–12 reflecting overall lesion severity. The lesions comprised edema (tissue swelling), erythema/hemorrhage (redness), excoriation (skin breakdown), and xerosis/scaling (dryness).

Auricular thickness was monitored in the central pinna region using a calibrated digital micrometer. Pruritus was quantified during video-recorded 15-min sessions (starting 24-h post-dose) by three independent observers, with scratching defined as intentional paw contact followed by rapid withdrawal from the lesional areas.

Histological analysis

Skin samples were fixed in 4% paraformaldehyde (24 h), embedded in paraffin, and cut into 5 µm sections that were stained with hematoxylin & eosin (H&E), then epidermal thickness was measured.

For each histologic section, epidermal thickness was measured at five randomly selected sites within three systematically sampled microscopic fields, encompassing the central and bilateral peripheral regions of the tissues [24]. Mast cells were identified by staining with toluidine blue (TB), and quantified in five randomly selected microscopic fields (200 × magnification) by two independent blinded observers. Data from all animals were aggregated, and group-level results are presented as means ± standard deviation (SD) [25].

RT-qPCR analysis

Total RNA was isolated from fresh skin tissues or from cells using SevenFast® Total RNA Extraction Kits (SevenBio) and purified. Complementary DNA was synthesized from 1 µg RNA using All-in-One cDNA Synthesis Kit II (SevenBio). The RT-qPCR reactions

Table 1 The primer sequences.

Gene	Forward primer (5′–3′)	Reverse primer (5′–3′)
IL-1β	TCCTCCGTTCCTTCATTCCTCAG	GAAAGAAAGTGGGTGGGCATCC
IL-4	GGTCTCAACCCCCAGCTAGT	GCCGATGATCTCTCTCAAGTGAT
IL-6	TAGTCCTTCCTACCCCAATTTCC	TTGGTCCTTAGCCACTCCTTC
IL-10	GCTCTTACTGACTGGCATGAG	CGCAGCTCTAGGAGCATGTG
IL-13	TCAGTGGGACAGGACGCAGTG	GGCTTGGCAGTAATCAGTGGTCAG
IL-17A	GATGCTGTTGCTGCTGCTGAG	TGGAACGGTTGAGGTAGTCTGAG
IL-31	CCAGTCTGCCTCCGCCTATC	CTTGGGACCGCTTAGATAACTTCAG
TNF-α	GCAACTGTTCCTGAACTCAACT	ATCTTTTGGGGTCCGTCAACT
IFN-γ	ATGAACGCTACACACTGCATC	CCATCCTTTTGCCAGTTCCTC
β-Actin	TTCTTCTGCCGTTCTCCCATAGG	CCACTTATCACCAGCCTCATTAGC

included 2 × SYBR Green qPCR MasterMix II (SevenBio) and proceeded on an Mx3000P system (Agilent Technologies Inc., Sana Clara, CA, USA). Table 1 shows the gene-specific primers (Sangon Biotech, Shanghai, China) and their sequences. Gene expression was normalized to β-actin using the $2^{-\Delta\Delta Ct}$ method, and melting curve analysis confirmed primer specificity.

Enzyme-linked immunosorbent assay (ELISA)

Skin lesion tissues were briefly rinsed with ice-cold phosphate-buffered saline (PBS; 0.01 M, pH 7.4) to remove residual blood. Wet tissue weight was recorded, then the tissues were finely minced and homogenized using a Servicebio mechanical tissue homogenizer (Servicebio, Wuhan, China) in PBS containing protease inhibitors (1:9 w/v tissue-to-buffer ratio). The homogenate was centrifuged at 12,000 × *g* for 15 min at 4 °C, and supernatants were collected to quantify TNF-α (#SEKM-0034), IL-1β (#SEKM-0002), IL-6 (#SEKM-0007), IL-10 (#SEKM-0010), IL-13 (#SEKM-0014) and IL-31 (#SEKM-0320; all from Solarbio Science & Technology Co., Ltd., Beijing, China).

RESULTS

Characterization of SVP and CGP

We purified polysaccharide fractions from SVP and CGP with carbohydrate contents of 85.3% and 80.8%, respectively. Extraction yields for SVP and CGP were 1.5% ± 0.14% and 2.29% ± 0.28%, respectively. UV spectral analysis confirmed high purity, with no absorbance peaks at 260 or 280 nm for either SVP or CGP polysaccharides (Fig. 1A,B), indicating undetectable levels of protein or nucleic acid contaminants. The FT-IR spectroscopy revealed very similar structural profiles between SVP and CGP (Fig. 1C,D), which were characteristic of typical polysaccharides, including broad O–H stretching at 3417 cm^{-1}, weak aliphatic C–H stretching at 2925 cm^{-1}, and prominent C–O–C/C–O absorption at 1078 cm^{-1} (glycosidic bonds/pyranose rings). The SEM findings revealed distinct morphological features of the SVP and CGP polysaccharides (Fig. 1E,F), as SVP exhibited a relatively continuous and smooth morphology, suggesting a more compact structure, while CGP displayed a looser and rougher texture.

SVP and CGP attenuate LPS-induced inflammatory responses in macrophages

We assessed the cytotoxicity of the SVP and CGP polysaccharides in RAW264.7 macrophages. Fig. 2A shows that the polysaccharides did not affect RAW264.7 cell viability at concentrations up to 200 μg/ml vs. untreated controls. Macrophages are key immune mediators that secrete pro-inflammatory mediators upon activation (cytokines such as TNF-α and IL-1β) that promote inflammation [26]. We evaluated the anti-inflammatory potential of SVP and CGP using a standardized inflammatory model *in vitro* consisting of RAW264.7 murine macrophages stimulated with lipopolysaccharide (LPS). Anti-inflammatory effects were assessed by analyzing NO production and profiling inflammatory cytokines. Fig. 2B shows that LPS stimulation significantly elevated NO production compared to unstimulated controls ($p = 0.000014$). Both SVP and CGP at concentrations ranging from 25 to 200 μg/ml significantly and dose-dependently suppressed LPS-induced NO secretion in RAW264.7 cells.

Fig. 2C,D shows the RT-qPCR results of the pro-inflammatory cytokines TNF-α and IL-1β. Stimulation with LPS significantly upregulated TNF-α and IL-1β expression compared with controls. Both SVP and CGP (at 200 μg/ml) significantly reduced IL-1β and TNF-α expression, indicating that SVP and CGP exert anti-inflammatory effects in activated macrophages.

Preparation and characterization of SVP and CGP-hydrogels

We prepared SVP and CGP-hydrogels (Fig. 3A) and visualized their structures using SEM (Fig. 3B). The blank hydrogel had dense aggregates with uniform block-like clustering, whereas SVP-hydrogel displayed a porous, interconnected fibrillar network. The CGP-hydrogel showed rough surfaces with small, dense pores compared to the SVP-hydrogel. Quantitative analysis of SEM micrographs using ImageJ confirmed that mean pore diameters were significantly

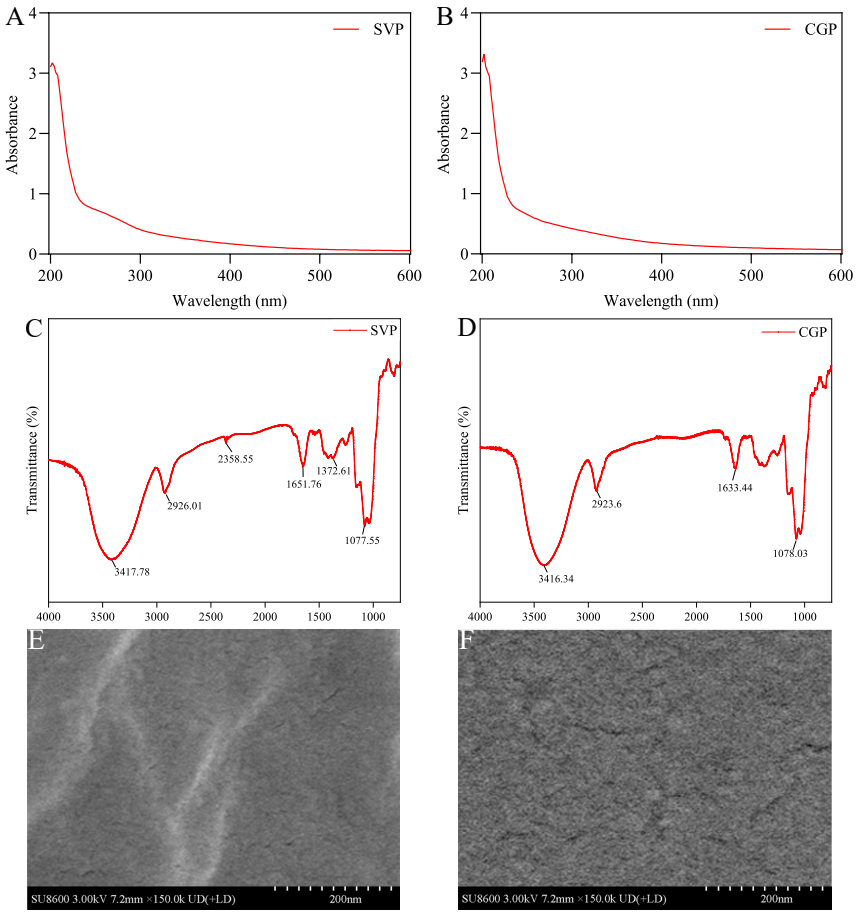

Fig. 1 Characterization of SVP and CGP. UV spectra of (A) SVP, (B) CGP. FT-IR spectra of (C) SVP, (D) CGP. SEM of (E) SVP, (F) CGP.

longer ($p = 0.00157$) in SVP than in CGP-hydrogels (56.26 ± 5.34 vs. 10.35 ± 1.45 µm; $p = 0.00157$). Therapeutic strategies for AD emphasize the critical role of sustained epidermal hydration in facilitating barrier repair. The clinical efficacy of hydrogels is closely linked to their moisture retention properties [27]. Therefore, the water retention capacities of the three hydrogels were evaluated. Fig. 3C shows that hydration maintenance was the best for SVP, compared with CGP and blank hydrogels. The enhanced moisturizing capacity of the SVP-hydrogel likely stems from SVP having stronger dipole-water molecular interactions.

SVP and CGP-hydrogels improved DNFB-induced atopic dermatitis

Compared to the controls, the frequency of scratching significantly increased in model mice within 15 min ($p = 0.000025$). Both SVP and CGP-hydrogel treatments attenuated this behavior, but SVP did so more effectively ($p = 0.00048$ vs. control). Fig. 4B shows that the SVP and CGP-hydrogels significantly increased the body weight of AD-like mice compared to the model group (SVP, $p = 0.000031$; CGP, $p = 0.000061$). The therapeutic effects of SVP-hydrogel were better than those of the CGP-hydrogel (Fig. 4C). Fig. 4D shows AD-like lesions in each group characterized by erythema, pruritus, and crust formation on the dorsal skin. These clinical manifestations progressively intensified with repeated DNFB challenges in the model group. Treatment with SVP or CGP-hydrogel significantly reduced the development of AD-like lesions (Fig. 4E). Significant edema developed by day 7 in the ears of mice treated with DNFB mice vs. controls (Fig. 4F). The SVP and CGP-hydrogels both suppressed this progression (Fig. 4G), showing a statistically significant inhibition of auricular inflammation from day 13 onward.

SVP and CGP-hydrogels inhibit epidermal thickening and mast cell proliferation in mouse models of AD

Histopathological analysis using hematoxylin and eosin and TB staining revealed significant epidermal thickening and inflammatory infiltration in the models (Fig. 5A,B). The dorsal epidermis was 4.8-fold thicker in model mice challenged with DNFB than in controls

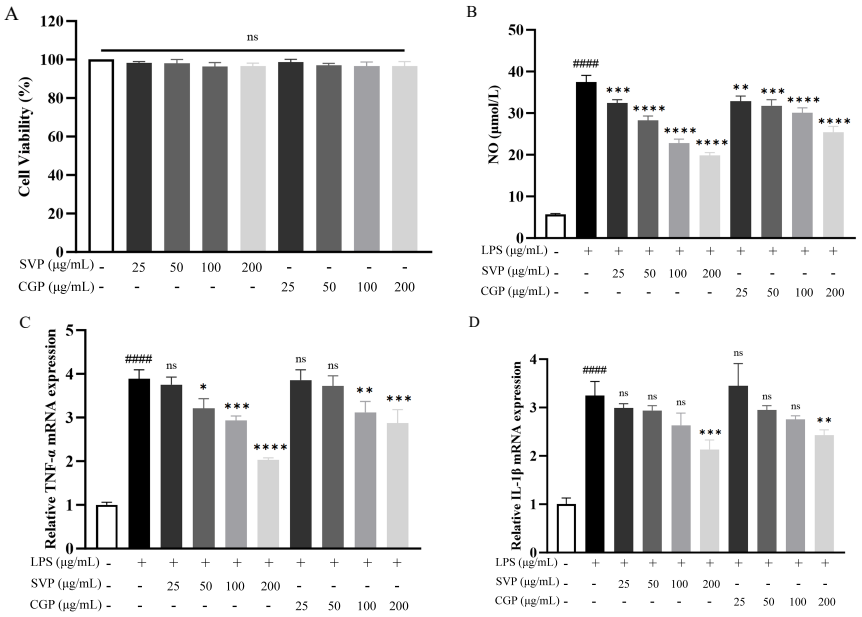

Fig. 2 Inflammatory responses in macrophages induced by LPS are attenuated by SVP and CGP. (A) Dose-response profiles of RAW264.7 cell viability after exposure to SVP and CGP; (B) Quantitative analysis of LPS-induced NO secretion after pretreatment with SVP and CGP. RT-qPCR analysis of (C) TNF-α and (D) IL-1β mRNA levels under LPS stimulation and SVP and CGP treatment. Each point represents means ± S.E.M. of three experiments. $^{\#\#\#\#}p < 0.0001$, compared with Control; * $p < 0.05$, ** $p < 0.01$, *** $p < 0.001$, **** $p < 0.0001$ vs. LPS; ns, not significant.

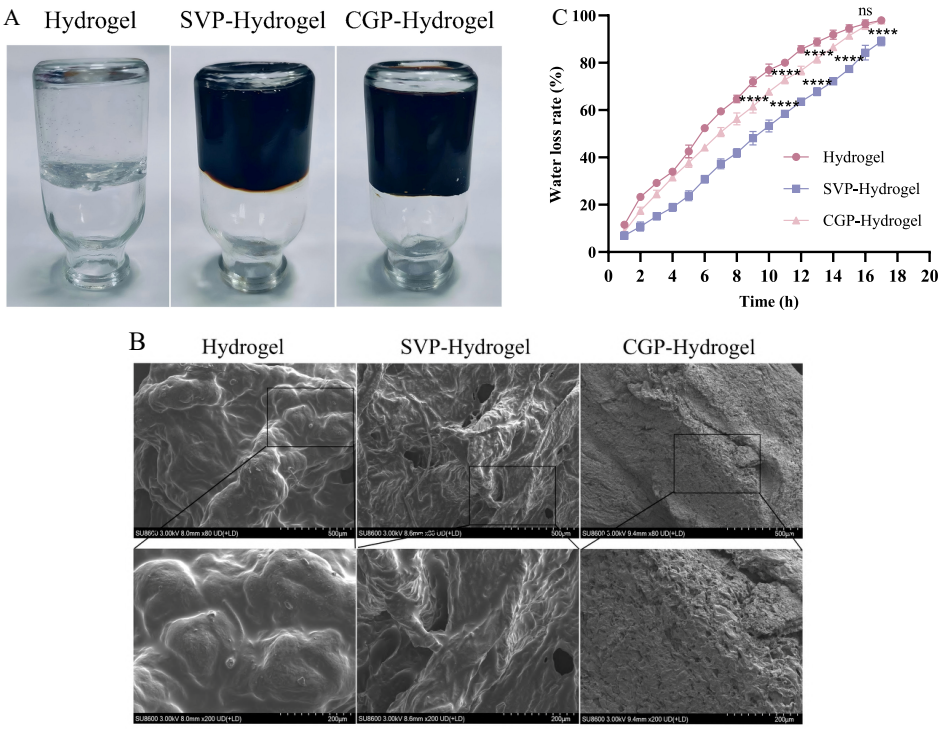

Fig. 3 Structural and functional characterization of SVP and CGP-hydrogels. (A) Visualization of hydrogels; (B) SEM images of three types of hydrogels; (C) Analysis of moisture retention capacity of three hydrogels. Points represent means ± S.E.M. of three experiments. *** $p < 0.001$, **** $p < 0.0001$ vs. hydrogels; ns, not significant.

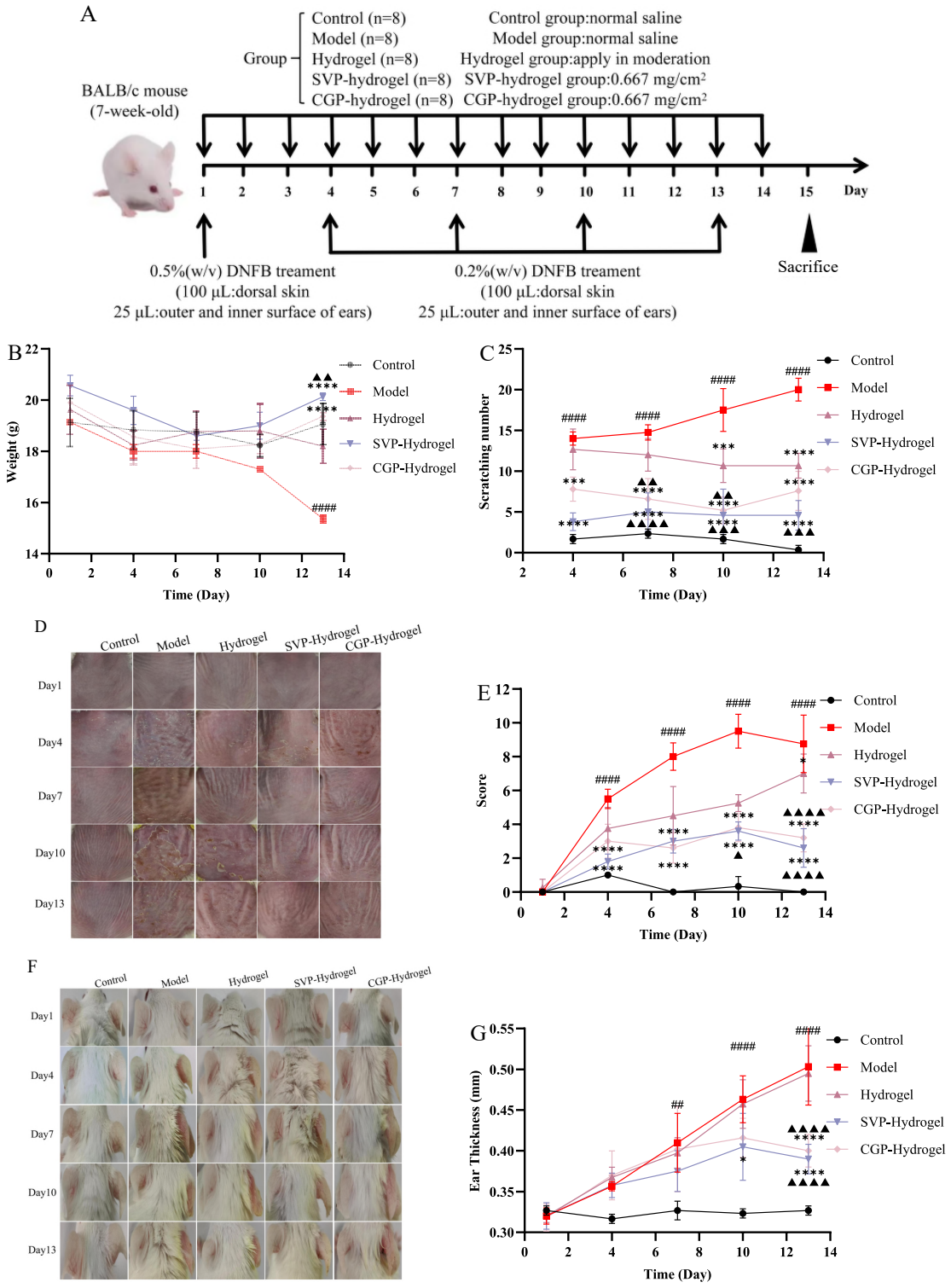

Fig. 4 Atopic dermatitis-like symptoms induced by DNFB in model mice were alleviated by SVP and CGP-hydrogels. (A) Schematic overview of experimental protocol; (B) Body weight of mice during experimental period; (C) Quantified 15-min scratching episodes; (D) Clinical photographs of lesional dorsal skin; (E) Composite severity scores quantified based on erythema, edema, excoriation, and scaling; (F) Clinical photographs of lesional right ears in each group; (G) Right ear thickness measured using a digital vernier caliper. Data are shown as means ± SD. ($n = 8$). $^{\#\#\#\#}p < 0.0001$ vs. control; $^{*}p < 0.05$, $^{***}p < 0.001$ vs. model; $^{\blacktriangle\blacktriangle}p < 0.01$, $^{\blacktriangle\blacktriangle\blacktriangle}p < 0.001$, $^{\blacktriangle\blacktriangle\blacktriangle\blacktriangle}p < 0.0001$ vs. hydrogels.

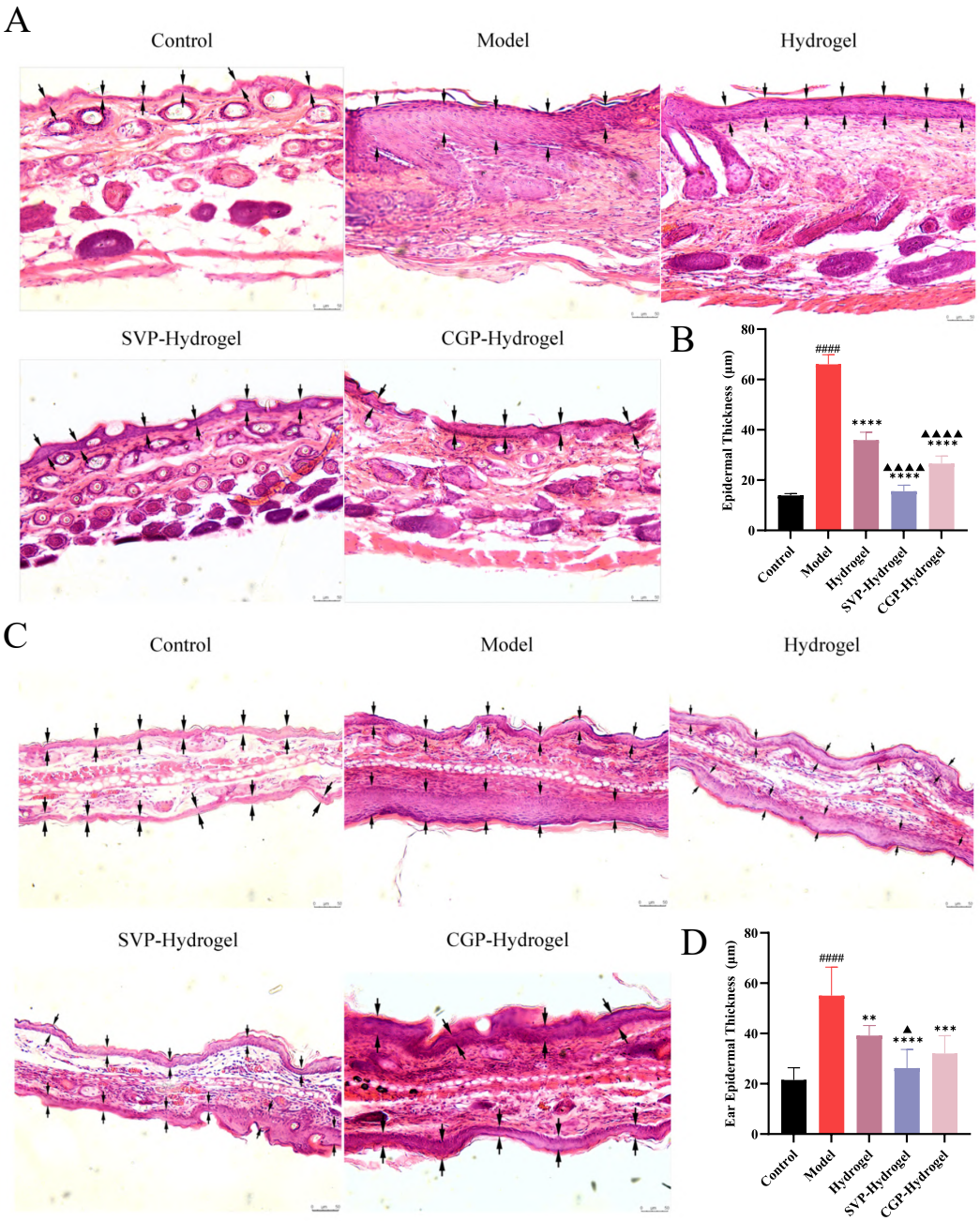

Fig. 5 Effect of SVP and CGP-hydrogels on the epidermal pathology in AD mice. (A) H&E staining showing dorsal skin epidermal thickness (black arrows; scale bar = 50 μm); (B) Quantitative statistic data of dorsal skin epidermal thickness; (C) H&E staining demonstrating ear epidermal dimensions (black arrows; scale bar = 50 μm; (D) Quantitative statistic data of ear epidermal thickness. The data were presented as means ± SD. ($n = 8$). Data are shown as means of 5 replicate measurements per sample. $^{\#\#\#\#}p < 0.0001$, vs. control; $^{**}p < 0.01$, $^{****}p < 0.0001$ vs. model; $^{▲▲}p < 0.01$, $^{▲▲▲}p < 0.001$, $^{▲▲▲▲}p < 0.0001$ vs. hydrogels.

(66.04 ± 6.6 vs. 13.88 ± 1.23 μm; $p = 0.000052$), indicating characteristic hyperkeratosis and hyperplasia. Both polysaccharide hydrogels significantly reversed these pathological changes: SVP-hydrogel restored skin thickness to 15.58 ± 3.65 μm ($p = 0.0000322$ vs. model; $p = 0.000075$ vs. blank hydrogel). The CGP-hydrogel achieved 23.58 ± 4.65 μm ($p = 0.000065$ vs. Model; $p = 0.000094$ vs. Hydrogel). The SVP-hydrogel more effectively reduced thickness by 58% more than the CGP-hydrogel. Therapeutic effects were consistently good in auricular tissues (Fig. 5C,D). Epidermal thickness in the ears of model mice increased 2.6-fold

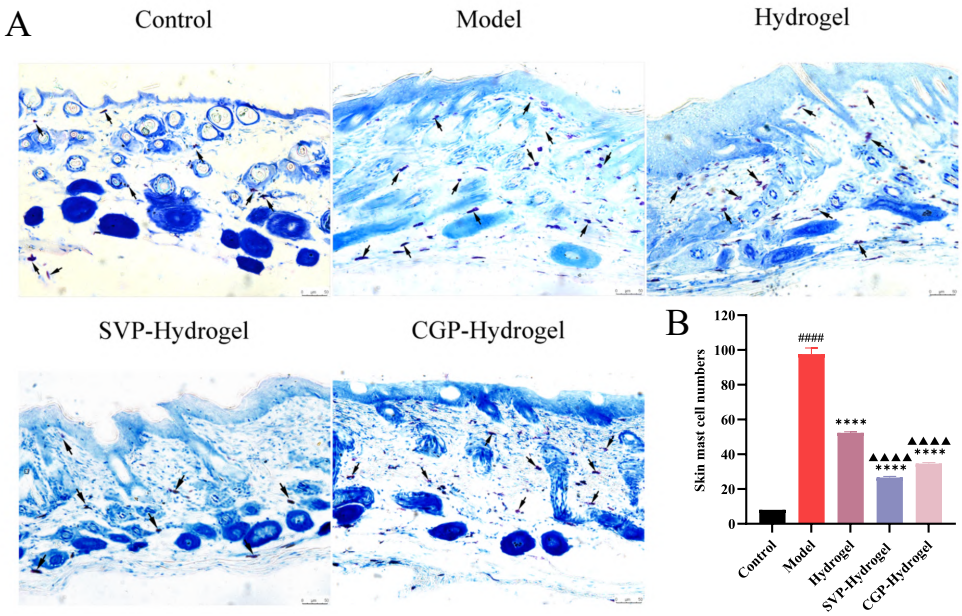

Fig. 6 Therapeutic suppression of mast cell infiltration in mouse models of AD. (A) Dermal mast cell clusters stained with Toluidine blue (black arrows; scale bar = 50 μm); (B) Data are presented as means ± SD ($n = 8$) from five replicate measurements per sample. $^{\#\#\#\#}p < 0.0001$, vs. control; $^{****}p < 0.0001$ vs. model; $^{▲▲▲▲}p < 0.0001$ vs. hydrogels.

vs. controls (55.03 ± 8.15 vs. 21.49 ± 8.15 μm; $p = 0.000046$), and the SVP-hydrogel restored this to near-normal levels, which was more effective than the CGP-hydrogel (26.26 ± 8.95 vs. 32.05 ± 13.27 μm).

Mast cell infiltration is a hallmark of AD pathology that is mediated through IgE/FcεRI signaling pathways [28]. Mast cell activation is associated with inflammatory responses in the skin [29]. Fig. 6 shows that the number of mast cells was significantly increased in the dermis of the model, compared with controls. In contrast, both SVP ($p = 0.00000162$ vs. Model, $p = 0.0000757$ vs. Hydrogel) and CGP-hydrogels ($p = 0.000007$ vs. Model) substantially reduced mast cell counts in dorsal and auricular skin. The inhibitory effects were stronger with SVP than with CGP hydrogels. This histomorphological evidence confirmed that the SVP and CGP-hydrogels suppressed inflammatory infiltration and normalized epidermal architecture.

SVP and CGP-hydrogels regulate the expression of inflammation-related cytokines in the skin tissues of AD mice

Compared to the controls, proinflammatory cytokines (TNF-α, IL-1β, IL-6) were upregulated, whereas anti-inflammatory IL-10 was suppressed in mice with DNFB-induced AD. The anti-inflammatory activity of the SVP-hydrogel was more effective than that of the CGP- and blank hydrogel, which indicated dichotomous regulation. The RT-qPCR finding revealed significant cytokine modulation in dorsal skin tissues after hydrogel treatment (Fig. 7). These transcriptional changes were universally confirmed at the protein level by ELISA. The SVP-hydrogel preferentially suppressed IL-31, which is a key mediator of pruritus pathogenesis ($p = 0.0000026$ and $p = 0.0000058$ vs. model and blank hydrogel). These molecular improvements correlated with histopathological recovery, confirming that SVP-hydrogel has dual anti-inflammatory and antipruritic activity for managing AD.

SVP and CGP-hydrogels modulate secretion of Th1/Th2/Th17-associated cytokines

The pathogenesis of AD involves dysregulation of Th1/Th2 cytokine balance and Th17-mediated inflammation. The RT-qPCR results revealed changes in key cytokines associated with Th1 (TNF-α, IFN-γ), Th2 (IL-4, IL-13), and Th17 (IL-17) pathways in the mice challenged with DNFB compared to controls ($p < 0.0001$; Fig. 7M–O). Both SVP and CGP-hydrogels attenuated Th2-associated cytokine expression, but the reduction was greater for the SVP, than the CGP-hydrogel (IL-4, $p = 0.045$ and IL-13 $p = 0.0007$ vs. blank hydrogel). The SVP-hydrogel also had broader modulatory effects on Th1/Th17-associated cytokines than the CGP-hydrogel. The IL-17 reduction with SVP-hydrogel ($p = 0.015$ vs. model) coincided with histopathological improvements (Figs. 5 and 6), indicating an association between cytokine modulation and symptom alleviation. These cytokine-level alterations suggest potential immunomodulatory activity, though cellular balance assessment would be required for definitive mechanistic confirmation.

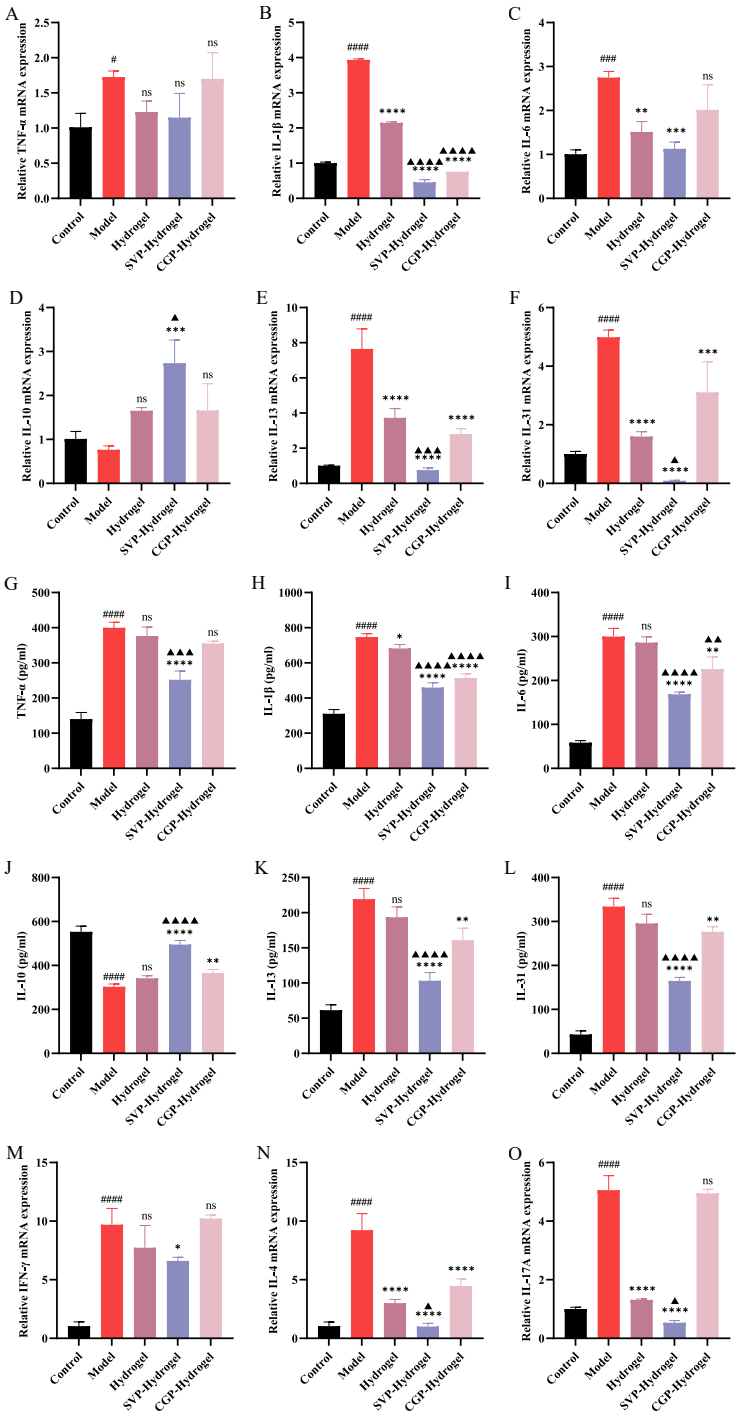

Fig. 7 Cytokine profile modulation by SVP and CGP-hydrogels in AD pathophysiology. (A) The relative mRNA expression of (A) TNF-α, (B) IL-1β, (C) IL-6, (D) IL-10, (E) IL-13, (F) IL-31, (M) IFN-γ, (N) IL-4, and (O) IL-13. Cytokine levels determined by ELISA kit (G) TNF-α, (H) IL-1β, (I) IL-6, (J) IL-10, (K) IL-13, and (L) IL-31. Results are expressed as means ± standard deviation ($n = 8$); $^{\#\#\#\#}p < 0.0001$ vs. control; $^{*}p < 0.05$, $^{**}p < 0.01$, $^{***}p < 0.001$, $^{****}p < 0.0001$ vs. model; $^{\blacktriangle}p < 0.05$, $^{\blacktriangle\blacktriangle\blacktriangle}p < 0.001$, $^{\blacktriangle\blacktriangle\blacktriangle\blacktriangle}p < 0.0001$ vs. hydrogels; ns, not significant.

DISCUSSION

AD is a chronic inflammatory skin disorder characterized by recurrent relapses, significantly impairing the quality of patients' lives. Although topical glucocorticoids remain the first-line treatment, their prolonged use is associated with cutaneous atrophy and other side effects. While conventional emollients effectively restore skin barrier function, they have limited ability to suppress inflammatory responses [30, 31]. This therapeutic gap has driven more research efforts to identify natural bioactive substances as safe alternatives to synthetic compounds. Fungal polysaccharides have significant anti-inflammatory and immunomodulatory activities. The high safety profile of fungal biopolymers offers a unique therapeutic potential for AD management through their dual capacity to modulate immune responses and maintain cutaneous homeostasis [32].

Topical application is the most effective drug delivery modality for AD management because it enables direct therapeutic access to lesional microenvironments [33]. Compared to traditional topical cream formulations, hydrogels offer distinct advantages through their unique biomaterial properties: a hydrating matrix that mimics the natural aqueous environment of skin, tunable viscoelasticity ensuring epidermal conformability, and an occlusive barrier function that prevents secondary infections. These characteristics synergistically confer superior moisturization for skin barrier restoration, enhanced cutaneous permeation, and reduced local irritation compared with traditional topical systems [34]. Carboxymethyl chitosan (CMCS) is a water-soluble derivative that exhibits potent antimicrobial activity and promotes wound healing by enhancing fibroblast proliferation and reducing scar formation [35]. Building on these properties and the historical records of anti-inflammatory fungi in Materia Medica, we developed composite hydrogels containing CMCS with SVP and CGP. We then evaluated the therapeutic potential of these fungal polysaccharide formulations for managing AD.

Here, we extracted and purified the fungal polysaccharides, SVP and CGP, conducted preliminary structural characterization of both, and prepared SVP and CGP-hydrogels. We investigated the effects of SVP and CGP-hydrogels on mouse models of AD induced by DNFB. We found that intervention with SVP and CGP-hydrogels significantly attenuated disease progression. Compared to the AD models, mice treated with SVP and CGP-hydrogels had thinner skin and reduced dermatitis severity scores. Histopathological analysis revealed that the SVP and CGP-hydrogels decreased epidermal hyperplasia and dermal inflammatory cell infiltration. The RT-qPCR and ELISA results showed that SVP and CGP-hydrogels significantly downregulated the expression of pro-inflammatory TNF-α, IFN-γ, IL-1β, and IL-6 and upregulated the anti-inflammatory IL-10.

Macrophages are pivotal components of the immune system, and are correlated positively with aggregation density and the severity of AD progression. Excessive NO production by immunocytes during inflammatory cascades potentiates localized tissue damage and promotes chronic inflammation [36]. Both SVP and CGP attenuated LPS-induced inflammatory responses in macrophages by reducing NO release and downregulating the secretion of pro-inflammatory cytokines. Macrophages express various polysaccharide recognition receptors, including the toll-like receptor (TLR) family, mannose receptor (MR) family, C-type lectins, complement receptor 3 (CR3), and scavenger receptors. Notably, TLR4 binds polysaccharides containing β-(1,3)-, β-(1,4)-, and α-(1,4)-glucan structures and modulates downstream inflammatory pathways [37]. Given the structural features of SVP and CGP, we theorize that these polysaccharides could target macrophages, suppress inflammation, and ameliorate AD symptoms through this mechanism. This preliminary mechanistic interpretation will be validated in subsequent studies exploring polysaccharide-macrophage interactions.

Hapten DNFB disrupts the cutaneous barrier and binds to keratinized proteins to form complete antigens. These neoantigens are recognized by epidermal Langerhans cells, which subsequently activate CD4+ T lymphocytes via antigen presentation, thereby initiating an immune response [38]. Upregulated pro-inflammatory cytokines facilitate the differentiation of naïve T lymphocytes into Th2 phenotypes, thereby disrupting Th1/Th2 homeostasis. This skewed polarization enables Th2-derived IL-4 and IL-13 to mediate IgE class switching in B lymphocytes, culminating in antigen-specific IgE synthesis [38]. Subsequent IgE crosslinking with high-affinity receptors (FcεRI) on mast cells triggers degranulation cascades, resulting in the liberation of preformed allergic mediators such as histamine, pleiotropic cytokines, and proteolytic enzymes that exacerbate immune dysregulation [39].

Mechanistically, SVP and CGP potentially engage pattern recognition receptors on macrophages and keratinocytes, thus attenuating the secretion of key pro-inflammatory TNF-α, IL-1β, and IL-6. This immunomodulatory activity modulates cytokine profiles associated with Th1/Th2/Th17 pathways by suppressing Th2-associated cytokines (IL-4, IL-13), downregulating Th1 (IFN-γ) and Th17 (IL-17) mediators, and elevating anti-inflammatory IL-10. Both SVP and CGP-hydrogels significantly reduced concentrations of IL-31, a pruritogenic cytokine produced by macrophages and Th2 cells. Our data further revealed attenuated IL-17 production, which aligned with established cytokine modulation strategies [40]. While these cytokine alterations correlate with therapeutically improved AD symptoms and histopathology, future studies of T-cell subpopulations are warranted to confirm whether hydrogels directly remodel Th1/Th2/Th17

immune equilibrium.

Compared to clinical hormone therapies for AD, natural polysaccharide hydrogels offer distinct advantages such as reduced risk of hormone dependence and cutaneous atrophy, enhanced biocompatibility with therapeutic compounds, and integrable antimicrobial properties that mitigate resistance development. These biomaterial characteristics render hydrogel technology a promising therapeutic alternative for AD [34]. We showed that SVP-hydrogel significantly ameliorated AD symptoms and surpassed control hydrogels through multi-mechanistic actions. These findings establish SVP-hydrogel as promising natural candidates for localized AD management. However, the absence of direct benchmarks against first-line clinical therapeutics precludes definitive assessment of effectiveness relative to current standards. Polysaccharide production yields require optimization for scalable translation. Future work should focus on optimizing extraction protocols and conducting rigorous comparative studies with established clinical therapies to comprehensively evaluate therapeutic potential. These advancements will advance SVP-hydrogel toward clinical translation while providing foundational evidence for novel AD treatment strategies.

Acknowledgements: This work was supported by the Jilin Provincial Scientific and Technological Development Program (Grant No. 20250102332JC).

REFERENCES

1. Langan SM, Irvine AD, Weidinger S (2020) Atopic dermatitis. *Lancet* **396**, 345–360.
2. Mandlik DS, K. MS, and Patel SS (2021) Sarsasapogenin and fluticasone combination improves DNFB induced atopic dermatitis lesions in BALB/c mice. Immunopharmacol Immunotoxicol **43**, 767–777.
3. Callewaert C, Knödlseder N, Karoglan A, Güell M, Paetzold B (2021) Skin microbiome transplantation and manipulation: Current state of the art. *Comput Struct Biotechnol J* **19**, 624–631.
4. Chovatiya R, Paller AS (2021) JAK inhibitors in the treatment of atopic dermatitis. *J Allergy Clin Immunol* **148**, 927–940.
5. Adam DN, Gooderham MJ, Beecker JR, Hong CH, Jack CS, Jain V, Lansang P, Lynde CW, et al (2023) Expert consensus on the systemic treatment of atopic dermatitis in special populations. *J Eur Acad Dermatol Venereol* **37**, 1135–1148.
6. Zhang D, Wei Y, Zhu X, Zong L, Cui M, Li D, Zhang C (2025) Study on the intervention mechanism of *Ganoderma lucidum* polysaccharides in mice with atopic dermatitis. *Food Res Int* **221**, 117212.
7. Huang R, Zhang W, Hu Y, Xu J, Dong Z, Liu J, Zhou L (2025) *Houttuynia cordata* polysaccharides ameliorate atopic dermatitis in mice through modulation of skin immune barrier and lipid metabolism. *Int J Biol Macromol* **314**, 144264.
8. Zhang T, Rao X, Song S, Tian K, Wang Y, Wang C, Bai X, Liu P (2024) WLJP-025p, a homogeneous *Lonicera japonica* polysaccharide, attenuates atopic dermatitis by regulating the MAPK/NFκB/AP-1 axis via Act1. *Int J Biol Macromol* **256**, 128435.
9. Hussain Z, Thu HE, Shuid AN, Kesharwani P, Khan S, Hussain F (2017) Phytotherapeutic potential of natural herbal medicines for the treatment of mild-to-severe atopic dermatitis: A review of human clinical studies. *Biomed Pharmacother* **93**, 596–608.
10. Liu J, Song J, Chen W, Sun L, Zhao Y, Zong Y, He Z, Du R (2024) Assessment of cytotoxicity, acute, subacute toxicities and antioxidant activities (*in vitro*) of *Sanghuangporus vaninii* crude polysaccharide. *J Ethnopharmacol* **319**, 117284.
11. Zhang JJ, Li Y, Zhou T, Xu DP, Zhang P, Li S, Li HB (2016) Bioactivities and health benefits of mushrooms mainly from China. *Molecules* **21**, 938.
12. Cicha-Jeleń M, Muszynska B, Kala K, Sulkowska-Ziaja K (2024) Medicinal potential of the giant puffball mushroom *Calvatia gigantea* (Agaricomycetes): A review. *Int J Med Mushrooms* **26**, 13–25.
13. Shi Y, Chu J, Lin W, Li J, Hou D, Li L (2024) Genome sequence of a traditional medicinal edible fungus *Calvatia gigantea* CGMCC5.9. *Microbiol Resour Announc* **13**, e0103623.
14. Peng S, Yu L, Jiang M, Cao S, Wang H, Lu X, Tao Y, Zhou J, et al (2025) Canthaxanthin ameliorates atopic dermatitis in mice by suppressing Th2 immune response. *Int Immunopharmacol* **147**, 113975.
15. Haiming C, Yijing L, Bin T, Xiaoyu M, Hailun L, Meiting D, Ziqing L, Xuwei Z, et al (2025) Modulation of the gut-skin axis by polysaccharides: Mechanisms and therapeutic potential in immune-related skin diseases. *Carbohydr Polym* **369**, 124143.
16. Shui J, Yang S, Zhao Y, Qi D, Su Y, Bai J, Zhang S (2025) Advances and prospects of targeting research for polysaccharide based drugs: A review. *Carbohydr Polym Technol Appl* **9**, 100735.
17. Wang J, Li W, Jin Y, Ji H, Li W, Zhang W, Zhang L, Fu L (2025) *Sanghuangporus vaninii* polysaccharides attenuate ovalbumin-induced allergic rhinitis in mice by improving the Th1/Th2 lymphocyte balance. *Int J Biol Macromol* **329**, 147789.
18. Gan M, Wu JC, Gu Q, Zhu J, Li Q (2025) Physicochemical, structural and functional properties of polysaccharides extracted from dried longan with different pretreatments: A comparison study. *J Food Compos Anal* **147**, 108021.
19. Huang Y, Shi F, Wang L, Yang Y, Khan BM, Cheong KL, Liu Y (2019) Preparation and evaluation of *Bletilla striata* polysaccharide/carboxymethyl chitosan/Carbomer 940 hydrogel for wound healing. *Int J Biol Macromol* **132**, 729–737.
20. Gu F-L, He X-M, Huang R-S (2019) Skin antiaging attributes of the *Dendrobium huoshanense* polysaccharides. *Curr Topics Nutraceut Res* **19**, 176–180.
21. Matsui MS, Muizzuddin N, Arad S, Marenus K (2003) Sulfated polysaccharides from red microalgae have antiinflammatory properties *in vitro* and *in vivo*. *Appl Biochem Biotechnol* **104**, 13–22.
22. Suto H, Matsuda H, Mitsuishi K, Hira K, Uchida T, Unno T, Ogawa H, Ra C (1999) NC/Nga mice: A mouse model for atopic dermatitis. *Int Arch Allergy Immunol* **120**, 70–75.
23. Kim TH, Kim GD, Ahn HJ, Cho JJ, Park YS, Park CS

(2013) The inhibitory effect of naringenin on atopic dermatitis induced by DNFB in NC/Nga mice. *Life Sci* **93**, 516–524.
24. Medsger TA Jr, Benedek TG (2019) History of skin thickness assessment and the Rodnan skin thickness scoring method in systemic sclerosis. *J Scleroderma Relat Disord* **4**, 83–88.
25. Raja N, Naikodi S, Govindarajan A, Palanisamy K (2021) Toluidine blue staining of murine mast cells and quantitation by a novel, automated image analysis method using whole slide skin images. *J Histotechnol* **44**, 190–195.
26. Hou C, Chen L, Yang L, Ji X (2020) An insight into anti-inflammatory effects of natural polysaccharides. *Int J Biol Macromol* **153**, 248–255.
27. Hu S, Bi S, Yan D, Zhou Z, Sun G, Cheng X, Chen X (2018) Preparation of composite hydroxybutyl chitosan sponge and its role in promoting wound healing. *Carbohydr Polym* **184**, 154–163.
28. Numata T, Harada K, Nakae S (2022) Roles of mast cells in cutaneous diseases. *Front Immunol* **13**, 923495.
29. Sun Y, Zhu D, Qu L, Li M, Du W, Wang M, Zhang Y, Chen G, et al (2024) Inhibitory effects of catalpol on DNCB-induced atopic dermatitis and IgE-mediated mast cells reaction. *Int Immunopharmacol* **126**, 111274.
30. Bai X, Rao X, Wang Y, Shen H, Jin X (2023) A homogeneous *Lonicera japonica* polysaccharide alleviates atopic dermatitis by promoting Nrf2 activation and NLRP3 inflammasome degradation via p62. *J Ethnopharmacol* **309**, 116344.
31. Bieber T (2022) Atopic dermatitis: An expanding therapeutic pipeline for a complex disease. *Nat Rev Drug Discov* **21**, 21–40.
32. Cheong K-L, Chen Q, Aweya JJ, Ji XL, Zhong S, Tan K (2025) Trends in polysaccharide-based hydrogels for skin anti-aging and skin antioxidant. *Int J Biol Macromol* **319**, 145366.
33. Chen B-R, Hsu K-T, Li T-L, Chan Y-L, Wu C-J (2021) Topical application of fucoidan derived from *Cladosiphon okamuranus* alleviates atopic dermatitis symptoms through immunomodulation. *Int Immunopharmacol* **101**, 108362.
34. Wan L, Wang M, Song Y, Sun G, Zhang R, Chen Z, Zhou Y, Ma K, et al (2025) Multifunctional hydrogel for the treatment of atopic dermatitis: Current advances and translational challenges. *Eur J Pharm Sci* **214**, 107288.
35. Chang G, Dang Q, Liu C, Wang X, Song H, Gao H, Sun H, Zhang B, et al (2022) Carboxymethyl chitosan and carboxymethyl cellulose based self-healing hydrogel for accelerating diabetic wound healing. *Carbohydr Polym* **292**, 119687.
36. Hu R, Xu S, Ao C, Ma Y, Bao H, Ye S, Sun J, Yuan H, et al (2022) Extraction and evaluation of biological activities of a polysaccharide from *Allium mongolicum* Regel. *ScienceAsia* **48**, 340–347.
37. Ji C, Zhang Z, Chen J, Song D, Liu B, Li J, Liu R, Niu J, et al (2021) Immune-enhancing effects of a novel glucan from purple sweet potato *Ipomoea batatas* (L.) Lam on RAW264.7 macrophage cells via TLR2- and TLR4-mediated pathways. *J Agric Food Chem* **69**, 9313–9325.
38. Guedes S, Neves B, Vitorino R, Domingues R, Cruz MT, Domingues P (2017) Contact dermatitis: in pursuit of sensitizer's molecular targets through proteomics. *Arch Toxicol* **91**, 811–825.
39. Poto R, Quinti I, Marone G, Taglialatela M, de Paulis A, Casolaro V, Varricchi G (2022) IgG autoantibodies against IgE from atopic dermatitis can induce the release of cytokines and proinflammatory mediators from basophils and mast cells. *Front Immunol* **13**, 880412.
40. Peng F, Zong J, Zhao T, Shi P, Lu M, Qu X, Han X, Zhao L, et al (2023) Anti-inflammatory and immunomodulatory effects of polysaccharide extracted from Wuguchong (maggot) on 2,4-dinitrochlorobenzene-induced atopic dermatitis in mice. *Front Pharmacol* **14**, 1119103.